NEW TSUNAMI HAZARD ASSESSMENT OF CHAÑARAL, CHILE, AFTER THE COASTAL MORPHOLOGY CHANGES DUE TO THE 2015 RIVER FLOOD

Rafael Aránguiz, Universidad Católica Ssma Concepción and CIGIDEN, raranguiz@ucsc.cl
Pedro Henríquez, Universidad Católica Ssma Concepción, phenriquez@ing.ucsc.cl
Miguel Esteban, Waseda University, esteban.fagan@gmail.com
Takahito Mikami, tmikami@tcu.ac.jp
Rodrigo Cienfuegos, Pontificia Universidad Católica de Chile and CIGIDEN, racienfu@ing.puc.cl
Marco Quiroz, Pontificia Universidad Católica de Chile and CIGIDEN, mqquiroz@uc.cl

INTRODUCTION

Chañaral is a town located at the mouth of the Salado River in northern Chile (Lat 26.3 °S). The main economic activity in its vicinity is copper mining, such as at Potrerillos and El Salvador. The river mouth is typically closed due to the coastal sediment transport. In addition, a large reclamation area was built from mine tailings and a highway was constructed on an elevated levee in the reclamation area.

Furthermore, Chañaral is under tsunami hazard, with the last tsunami event taking place in 1922. According to historical records, the tsunami reached 10 m (Soloviev & Go, 1975). This event occurred prior to the deposition of mine tailings, which started in 1930. The official tsunami inundation map was made in 2014, and the tsunami scenario considered an extreme event based on the 1922 tsunami plus a high tide (SHOA, 2014). The maximum tsunami runup was estimated to be 17 m.

In March 2015, a heavy rain event took place over the Atacama Desert and a catastrophic flood affected Chañaral, with a maximum water depth of 4.5 m (Wilcox et al., 2016), significantly changing the coast. In fact, the elevated highway was destroyed and there was substantial coastal erosion.

The present work assesses the tsunami hazard considering the new coastal morphology, given that coastal erosion would allow a tsunami to easily surge into the river and subsequently the town.

METHODOLOGY

Bathymetric and topographic information prior to the 2015 river flood was collected in order to analyze the tsunami inundation before the river flood event. In addition, new topography and bathymetry data from after the 2015 river flood was collected in August 2017, from which the new coastal morphology was obtained.

The tsunami inundation area was assessed by means of tsunami numerical simulations. The tsunami scenario is the same as that in the tsunami inundation maps from SHOA (SHOA, 2014), which consider a 1922-like event of magnitude Mw 8.3. This event considered the following parameters: rupture length L=380km, rupture width W=130km, uniform slip D=8m and strike, dip and rake angles of 9°, 20° and 90°, respectively. The reference point (south western corner) of the fault was defined at the coordinates 27.03°S, 71.65°W with a focal depth of 10km. The rise time is defined to be $t_{rise} = 60s$.

The tsunami simulations were carried out by means of the NEOWAVE model, which solves the non-linear shallow water equations with a vertical velocity term to account for weakly-dispersive waves and a momentum conservation scheme to describe flow discontinuities such as bores and hydraulic jumps (Yamazaki et al., 2011; 2009). Five levels of nested grids were used, with resolutions of 120" (~3.7km), 30"(~900m), 6"(~180m), 1"(~30m) and 0.333" (~10m). Level 1 and 2 grids were built from GEBCO bathymetric data, while levels 3 to 5 were derived from nautical charts. In addition, Level 5 grids incorporated new bathymetry and topography obtained after the 2015 flood event provided by the Ports Works Department of Ministry of Public Works. The simulation considered the maximum tide level as 1 m.

Figure 1 shows 3 out of 5 simulation grids obtained from the combined bathymetry and topography after the 2015 event. From the figure, it is possible to observe the two new coastal lagoons formed after the 2015 event.

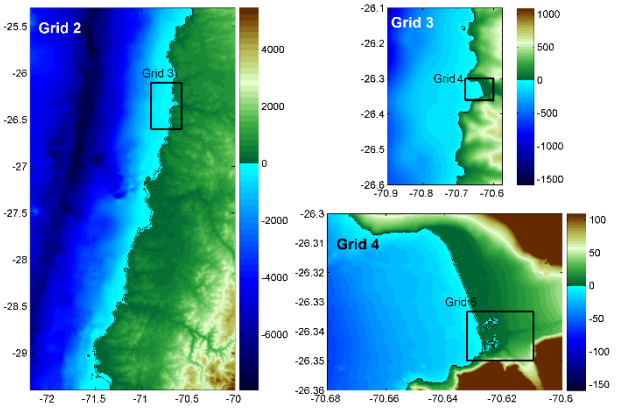

Figure 1. Nested grids used for tsunami numerical simulations of the 1922-like tsunami in Chañaral.

RESULTS

Figure 2 shows the generation and propagation of the 1922-like tsunami. Since $t_{rise} = 60s$, t=1 min represents the tsunami initial condition. It is possible to observe that due to the proximity of the trench to the coast, the first tsunami wave arrives within 12 min after the earthquake.

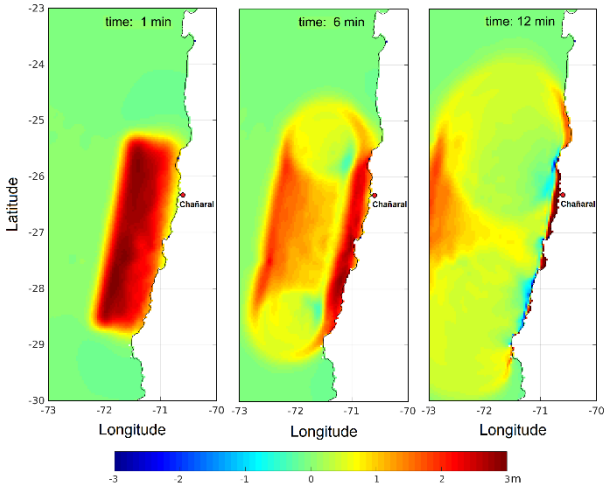

Figure 2. Snapshot of surface elevation.

Figure 3 shows the tsunami waveform at the tide gauge location. The sea level starts from 1m due to the tide level. It is possible to observe that the first tsunami wave reached up to 8m, with the second wave being the largest one. In addition, the third wave reached similar amplitude as the previous wave. This effect demonstrated the importance of tsunami resonance on tsunami wave amplification in Chañaral. Figure 4 shows the maximum simulated flow depth (a) and flow velocity (b) for the level 5 grid. The thin black lines represent contour lines of ground elevation every 5 m. Therefore, it is possible to observe that the tsunami surged into the river and reached a maximum runup of 15 m. In addition, the maximum flow depth is ~12 m at the coastline, and flow velocities are as large as 10 m/s.

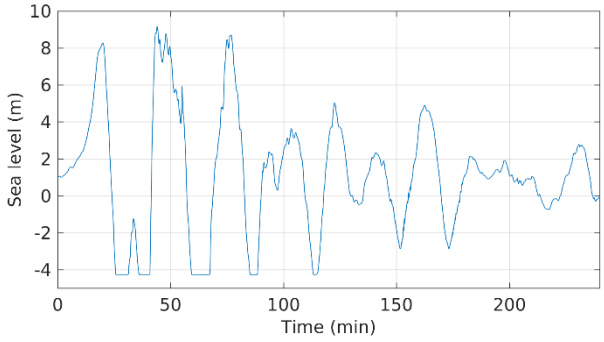

Figure 3. Tsunami waveform at tide gauge (*G at Figure 3).

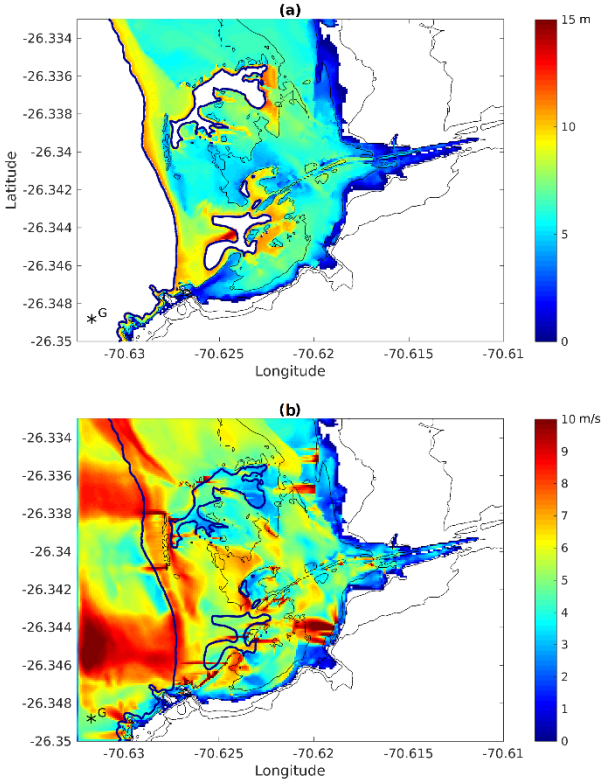

Figure 4. a) Maximum tsunami flow depth. b) Maximum tsunami flow velocity. Black thick line is the coastline, while thin lines are contour lines every 5 m.

Even though the maximum runup in the present analysis (15m) is lower than the runup computed by SHOA prior to the river flood (17m), these values are of the same order of magnitude. Therefore, the coastal erosion and morphology changes do not generate significant changes on tsunami inundation.

The aforementioned results, in combination with modal analysis, will allow possible future mitigation measures for both tsunami and river floods to be formulated. Since river flooding needs a direct discharge into the sea, the river mouth should be located in a zone with no significant tsunami wave amplification in order to avoid substantial flooding in case of a future tsunami. This analysis will be important when new tsunami mitigation measures are proposed, in order to increase the resilience of this community to such natural hazards.

CONCLUSIONS

The tsunami hazard in the study site was assessed by taking into account coastal morphology changes after the 2015 river flood event. The numerical simulations showed that maximum runup can reach up to 15 m and significant part of the coastal community can be flooded by the tsunami. It was also observed that the first tsunami wave can arrive within 15 min, and tsunami resonance can play an important role in tsunami wave amplification. The simulations indicate that three large waves could strike the town, with the second one being the largest. Finally, future mitigation measures for both tsunami and river flood should consider a multi-hazard risk assessment, due to the fact that both hazards behave in a completely different way.

ACKNOWLEDGEMENTS

The authors would like to thank CONICYT (Chile) for its FONDAP 15110017, and FONDECYT 11140424 grants. Thanks to the Faculty of Engineering at UCSC for the partial funding of the field survey.

REFERENCES

SHOA. (2014). Carta Inundación por Tsunami Chañaral. Servicio Hidrográfico y Oceanográfico de la Armada de Chile.

Soloviev, S. L., & Go, C. N. (1975). *A Catalogue of Tsunamis on the Eastern Shore of the Pacific Ocean*. Moscow: Nauka Publishing House.

Wilcox, A. C., Escauriaza, C., Agredano, R., Mignot, E., Zuazo, V., Otárola, S., … Mao, L. (2016). An integrated analysis of the March 2015 Atacama floods. *Geophysical Research Letters*, *43*, 8035-8043. http://doi.org/10.1002/2016GL069751

Yamazaki, Y., Cheung, K. F., & Kowalik, Z. (2011). Depth-integrated, non-hydrostatic model with grid nesting for tsunami generation, propagation, and run-up. *International Journal for Numerical Methods in Fluids*, *67*(12), 2081-2107. http://doi.org/10.1002/fld.2485

Yamazaki, Y., Kowalik, Z., & Cheung, K. F. (2009). Depth-integrated, non-hydrostatic model for wave breaking and run-up. *International Journal for Numerical Methods in Fluids*, *61*(5), 473-497. http://doi.org/10.1002/fld.1952